



Fretting wear characteristics of AISI 1040 steel alloy

Krishnamurti Singh*, Mayank Tiwari, Anirban Mahato

Department of Mechanical Engineering, Indian Institute of Technology, Patna, 801106, Patna, INDIA.

*Corresponding author: krishnamurti.pme16@iitp.ac.in

| KEYWORD | ABSTRACT |
|---|--|
| Fretting wear Stick-slip Optical profilometry | Most of the shrink fit joints, couplings, and fasteners of machine components are generally made up of AISI 1040 steel. These components are subjected to fretting wear due to vibrations induced by machine operation. Fretting wear test on AISI 1040 steel is performed with different normal loads in ambient condition using Rtec MFT 5000 tribometer. The effect of different normal loads on coefficient of friction, slip regime and wear profile are analyzed. The result reveals that normal load has a significant effect on fretting wear performance of AISI 1040 alloy. Optical micrograph obtained from optical microscope shows that with an increase in normal load, wear depth increases and transition of slip regime from gross slip to partial slip occurs. |

1.0 INTRODUCTION

In general, mostly the mechanical components have different types of contacts which are subjected to vibration during running condition. In case of vibration, the amplitude of sliding in contacts is very small, usually in the order of microns. Loss of material from contacting bodies due to short amplitude vibration is known as 'fretting wear.' The first evidence of fretting wear study was found in the article by Tomlinson, (1927) where the term fretting was not used. According to Tobi et al., (2017), a systematic study of fretting wear based on the analytical solution was performed by Cattaneo and independently by Mindlin. Fretting wear is categorized in three slip regimes, out of which partial slip regime is the most critical since in this regime, crack initiation and propagation takes place at the junction of the stick-slip zone. Vingsbo & Söderberg, (1988) presented a classical fretting map which represents the gross slip and partial slip regime as a function of normal load and sliding amplitude.

Received 30 June 2018; received in revised form 16 Aug 2018; accepted 25 Aug 2018.

To cite this article: Singh et al. (2019). Fretting wear characteristics of AISI 1040 steel alloy. Jurnal Tribologi 20, pp.65-73.

Johnson, (1985) presented the analytical expression for determining the distribution of normal and tangential traction, displacement in normal and tangential direction, slip distribution, stick-slip relation with normal and tangential traction.

In partial slip regime, the central region of the contact does not experience relative sliding, while in the gross slip regime, entire junction has a sliding motion, which is wear dominant. Li et al., (2017) conducted fretting wear test in a ball on plate configuration on Inconel 690 TT alloy. It was concluded that in gross slip regime, degradation mechanism was deformation, oxidation and delamination crack in worn subsurface, while in partial slip regime deformation of asperities in adhesion zone, oxidation at worn edge and fatigue crack at junction stick-slip.

With the increase in sliding amplitude, keeping normal load constant, the transition from partial slip to gross slip takes place. Li & Lu, (2013) performed fretting wear test on Inconel 600 alloy and concluded that with increase in sliding amplitude, coefficient of friction and wear volume increases. Jeong et al., (2007) conducted fretting wear test on AISI 1045 steel and concluded that coefficient of friction decreases with increase in normal load. Moreover, the transition from gross slip to partial slip was also observed.

Friction and wear behavior of bearing material under water contaminated compressor oil was investigated by Syahirah et al., (2015). It was reported that water contamination significantly affects the wear scar diameter.

Kumar and Wani, (2017) performed linear reciprocating wear test in hypereutectic Al-Si alloy/steel contact. The effect of normal load was investigated under dry and lubricated conditions. They have concluded that coefficient of friction was decreasing with the increase in load from 5-50N, later the value of COF increased for the load range of 50-80N and again the decrement in COF was observed for the load range of 80-100N. They have also shown that wear rate increased at the starting, later it decreased and then increased further with the normal load.

Fouvry et al., (1996) proposed the method for quantification of wear damage using dissipated frictional energy in the contact interface for different regimes of fretting and proposed transition criteria for various regimes of fretting.

AISI 1040 steel is used in the couplings, crankshaft and shrink fit joints where fretting wear is one of the important failure modes. It is observed from the literature, that marginal research on the fretting wear has been reported on AISI 1040 steel hence a detailed investigation is needed on AISI 1040 steel under gross and partial slip conditions.

In the present study of fretting wear experiment on AISI 1040 steel plate sliding against AISI 4340 steel pin is carried out at constant sliding amplitude and sliding frequency with different normal loading conditions in order to obtain the effect of normal load on the coefficient of friction and wear damage.

2.0 EXPERIMENTAL PROCEDURE

Before performing the fretting wear test, samples are polished up to the average surface roughness R_a of $0.03 \mu\text{m}$. Hardness tests are performed on both upper and lower samples using Vickers hardness tester (Zwick, USA). Figure 1a and 1b show the indentation mark of Vickers hardness test on upper and lower sample at 2 Kgf load respectively.

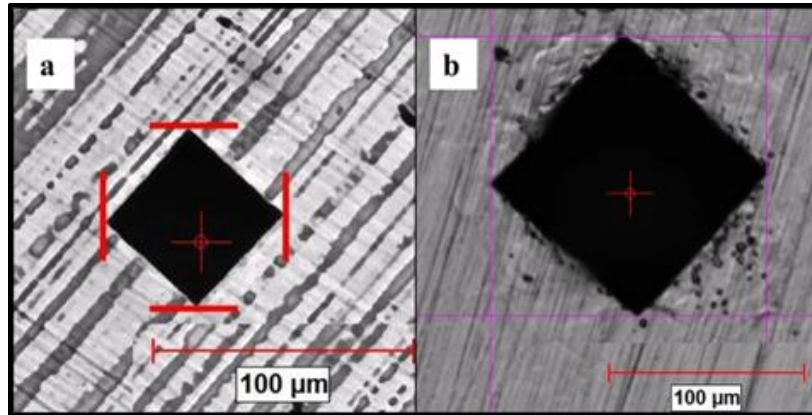


Figure 1: Optical micrograph of Vickers hardness test.

Figure 2 shows the stress-strain curve of AISI 1040 steel obtained from the tensile test conducted at a crosshead speed of 1.5mm/min. Yield strength is found to be 224 MPa obtained by 0.2% strain offset.

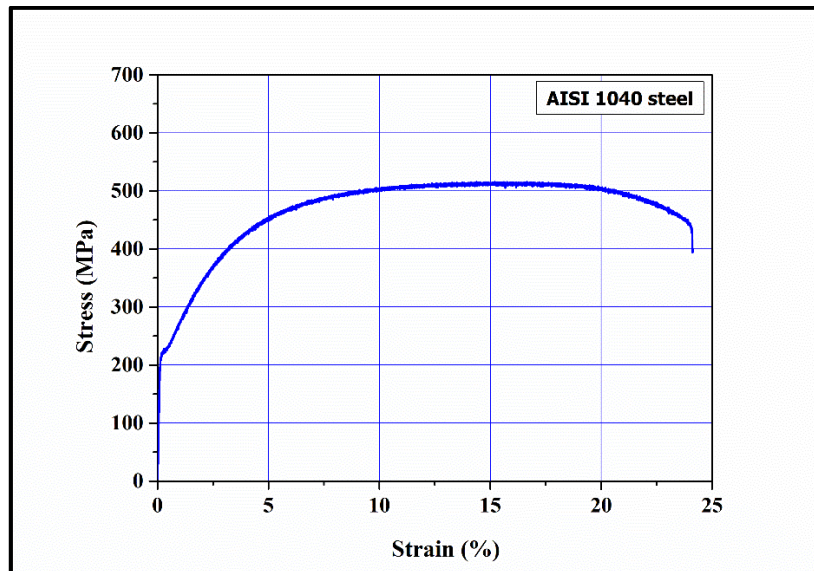


Figure 2: Stress strain graph of AISI 1040.

Fretting wear tests of AISI 1040 steel alloy are performed using Rtec multifunctional tribometer (Rtec Instruments, USA) in pin-on-plate contact configuration at room temperature under dry sliding condition. The target sample is lower specimen made up of AISI 1040 steel alloy plate with dimension 35×25×3 mm and the upper specimen is 6 mm diameter hemispherical pin of AISI 4340 steel. Figure 3 shows the schematic contact configuration.

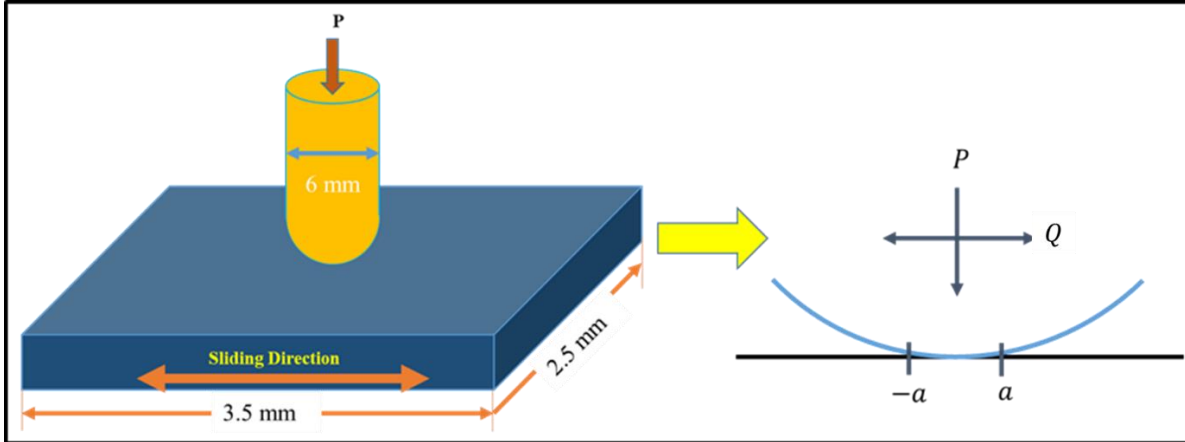


Figure 3: Schematic representation of pin on plate contact.

Fretting wear tests are performed at constant sliding amplitude 50 μm , constant sliding frequency 50 Hz and different normal load ranging from 10 N to 45 N at an incremental value of 5 N. Mechanical properties of the test materials are listed in Table 1.

Table 1: Mechanical properties of the materials

| Material | Modulus of Elasticity (GPa) | Poisson's Ratio | Hardness(HV) |
|-----------|-----------------------------|-----------------|--------------|
| AISI 1040 | 190 | 0.3 | 180 |
| AISI 4340 | 210 | 0.3 | 776 |

3.0 ANALYTICAL SOLUTION OF CONTACT MODEL

The hemispherical pin-on-plate configuration is widely used in the tribological investigation of contacting bodies. The solution of Hertzian point contact problem for sliding contact is well known. Brief details of fretting theories along with their solutions according to the contact configuration (see Figure 3), are summarized as follows:

The contact pressure distribution $p(x)$ according to the Hertzian theory Johnson, (1985) is given as:

$$p(x) = p_0 \left(1 - \frac{x^2}{a^2}\right)^{\frac{1}{2}} \quad (1)$$

Where, p_0 and a is maximum contact pressure and contact radius respectively. The analytical expressions for p_0 and a are written as:

$$a = \left(\frac{3PR}{4E^*}\right)^{\frac{1}{3}} \quad (2)$$

$$p_0 = \left(\frac{6PE^{*2}}{\pi^3 R^2} \right)^{\frac{1}{3}} \quad (3)$$

Where, E^* is the composite modulus of elasticity and R is the effective radius of contacting body.

$$\frac{1}{E^*} = \frac{1-\nu_1^2}{E_1} + \frac{1-\nu_2^2}{E_2} \quad (4)$$

$$\frac{1}{R} = \frac{1}{R_1} + \frac{1}{R_2} \quad (5)$$

With the application of the oscillating tangential displacement, contacting body experiences an oscillating frictional force. In case of gross slip condition, maximum tangential force (Q_{max}) is equal to the limiting frictional force P , where μ is coefficient of friction. Whereas, in case of partial slip condition, maximum tangential force is less than the limiting frictional force in central stick zone and sliding takes place at the boundary of the contact. Shear traction distribution in the stick-slip zone was presented by (Johnson, 1985) is given as:

$$q(x) = \begin{cases} \mu p_0 \left(1 - \frac{x^2}{a^2}\right)^{\frac{1}{2}}, & c \leq x \leq a \\ \mu p_0 \left(1 - \frac{x^2}{a^2}\right)^{\frac{1}{2}} - \mu p_0 \frac{c}{a} \left(1 - \frac{x^2}{c^2}\right)^{\frac{1}{2}}, & x \leq c \end{cases} \quad (6)$$

Where, c is the radius within which there is no relative motion. Partial slip takes place in region $c \leq x \leq a$. In partial slip regime, the stick-slip radius is related as.

$$\frac{c}{a} = \left\{ 1 - \frac{Q}{\mu P} \right\}^{\frac{1}{3}} \quad (7)$$

Pasanen et al., 1996 presented the method for obtaining maximum coefficient of friction in the fretting contact by measuring the stick and slip radius which can be expressed as follows :

$$\mu = \left(\frac{1}{1 - \left(\frac{c}{a}\right)^3} \right) \times \frac{Q_{max}}{P} \quad (8)$$

4.0 RESULTS AND DISCUSSION

Figure 4 shows the variation in average coefficient of friction with normal load at 50 Hz frequency. It has been observed that coefficient of friction decreases with increase in normal load. In gross slip regime decrease in coefficient of friction with normal load is steeper however, in partial slip regime it is less steep. This phenomenon is attributed to plastic deformation of the asperities and contribution of third body particles at higher load resulting in lesser resistance to sliding process. Similar trend for the variation of coefficient of friction was observed by Jeong et al., (2007) for AISI 1018.

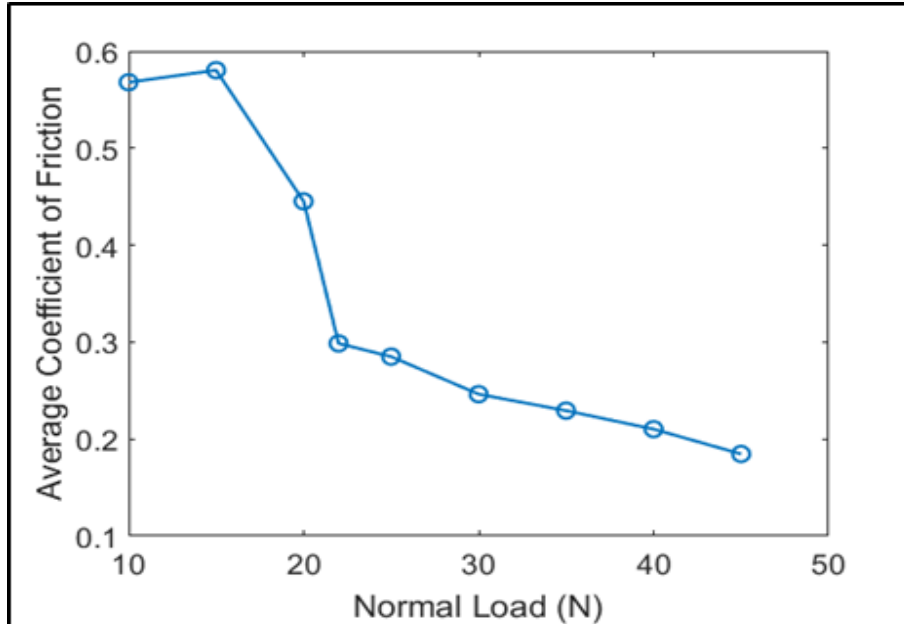


Figure 4: Variation of the coefficient of friction with normal load.

Figure 5 shows wear profile of the worn surface with normal load in partial slip regime. From the following figure, it is observed that wear depth increases with increase in normal load. A smooth profile in the central region shows that there is no sliding in the contact interface during entire test. During each applied stroke, the deformed material is accumulated around the stick zone and undergoes abrasion, micro cutting and fracture process which eventually provides rough profile around stick zone.

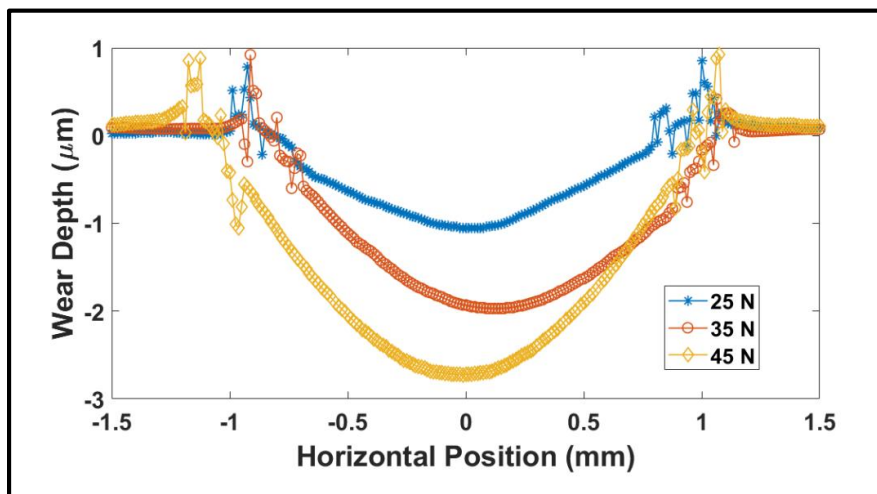


Figure 5: Wear profile in partial slip regime.

Figure 6 shows the worn surfaces obtained from the optical microscope in different sliding condition. From figure 6a, 6b and 6c it is observed that, gross sliding in the contact interface takes place for the applied load 10N, 15N and 20 N. After a load of 20 N, transition from gross sliding to partial sliding takes place. At 22 N normal load, visible stick zone in the center of the contact is observed with small scratches near the slip zone, which indicates that few wear debris are entrapped in the stick zone. These entrapped wear debris participated in sliding during the fretting process.

As the normal load increases from 22 N to 45 N, central stick zone expands, however a decrease in width of slip zone is observed. This phenomenon is there because, with an increase in normal load, sliding between two objects becomes difficult.

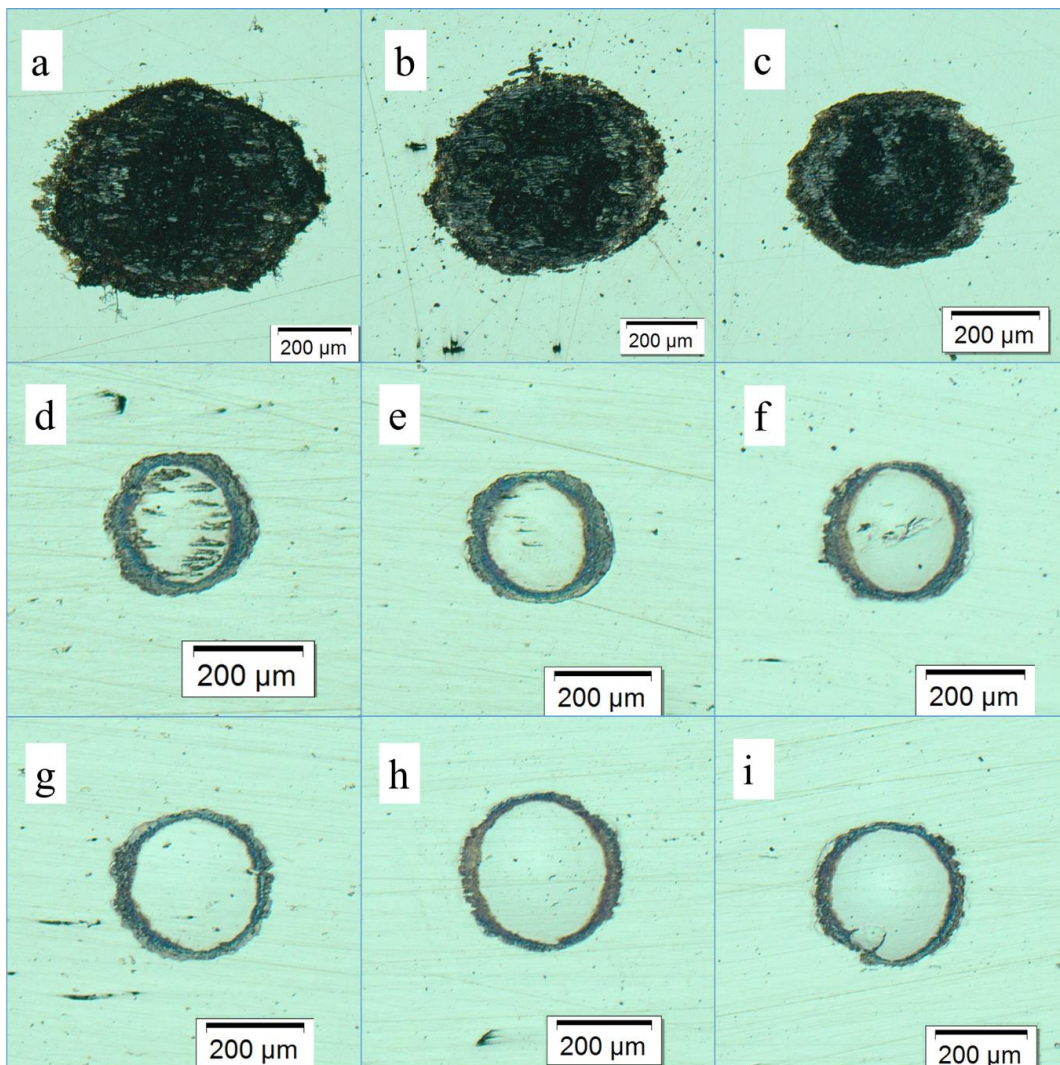


Figure 6: Optical micrographs of the worn scar at the applied normal load of (a) 10 N (b) 15 N (c) 20 N (d) 22 N (e) 25 N (f) 30 N (g) 35 N (h) 40 N (i) 45N.

Table 2 shows the comparison between experimentally and analytically obtained values of contact and stick dimensions. It can be seen that results are found to be close enough. There is small deviation because of the machine compliance and presence of relative slip between contacting bodies.

Table 2: Analytical and experimental results of contact.

| | | Load (N) | | | | |
|--------------|--------|----------|--------|--------|--------|--------|
| | | 25N | 30N | 35N | 40N | 45N |
| Experimental | 2a(mm) | 0.209 | 0.207 | 0.218 | 0.231 | 0.233 |
| | 2c(mm) | 0.139 | 0.148 | 0.176 | 0.194 | 0.183 |
| Analytical | 2a(mm) | 0.1607 | 0.1708 | 0.1795 | 0.1880 | 0.1995 |
| | 2c(mm) | 0.1167 | 0.1321 | 0.1407 | 0.1491 | 0.1660 |

Figure 7 shows the normalized shear traction distribution for 40 N applied normal load at the contact interface during fretting loading and unloading conditions. With the application of oscillating sliding motion, contact interface experiences shear traction due to friction between mating bodies. In partial slip condition, tangential traction is less than limiting frictional force as there is no relative slip. Maximum value of the shear traction is obtained at the inner boundary of slip zone where shear traction is equal to the limiting frictional force and it is zero at the extreme boundary of the contact. During unloading process, reverse relative slip (Johnson, 1985) takes place in between $c_1 \leq x \leq a$, where $c < c_1 < a$.

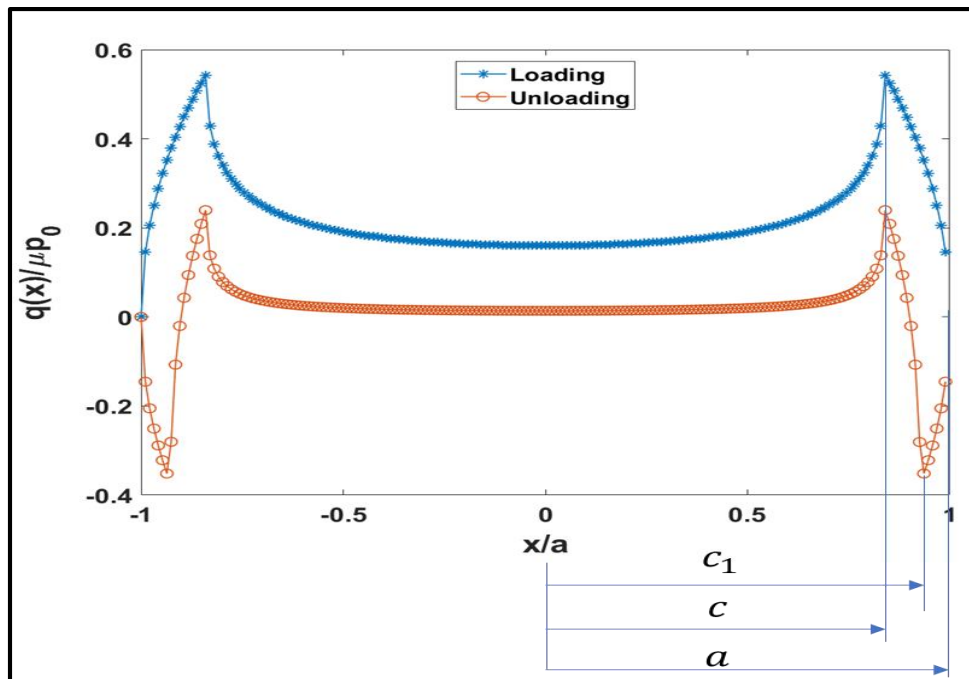


Figure 7: Shear traction distribution.

5.0 CONCLUSION

Fretting wear is one of the most surface damaging processes and contributes to bulk material failure. In the present work fretting wear experiment on AISI 1040 steel is carried out to obtain the effect of normal load on fretting wear behavior of AISI 1040 steel. Stick and slip dimensions are compared with the analytical result of the contact model. On the basis of result and discussion following conclusions are made:

1. With the increase in normal load, the coefficient of friction decreases. However, it is more significant in gross slip regime and attributed to the plastic deformation of asperities and contribution of third body particle at higher load.
2. Wear depth increases with increase in normal load in partial slip regime.
3. With the increase in normal load, transition of slip behavior from gross slip condition to partial slip condition takes place.
4. With the increase in normal load width of the slip region decreases.
5. Experimentally obtained contact dimensions are well correlated with the analytical results of the fretting contact.

ACKNOWLEDGEMENT

The authors gratefully acknowledge Department of Mechanical Engineering, Indian Institute of Technology Patna for providing the experimental facility.

REFERENCES

- Tomlinson G. A. (1927). The Rusting of Steel Surfaces in Contact. *Proceeding of the Royal Society of London*, 115(771), 472-483.
- Tobi A. L., Sun W., & Shipway P. H. (2017). Investigation on the plasticity accumulation of Ti-6Al-4V fretting wear by decoupling the effects of wear and surface profile in finite element modelling, *Tribology International*, 113, 448-459
- Vingsbo, O., & Söderberg, S. (1988). On fretting maps. *Wear*, 126(2), 131-147.
- Johnson K. L. (1985). *Contact mechanics*. Cambridge University Press.
- Li, J., B.B. Yang, Lu, Y. H., Xin, L., Wang, Z. H., & Shoji, T. (2017). The degradation mechanism of Inconel 690TT induced by fretting wear in air. *Tribology International*, 116, 147-154.
- Li, J., & Lu, Y. H. (2013). Effects of displacement amplitude on fretting wear behaviors and mechanism of Inconel 600 alloy. *Wear*, 304(1-2), 223-230
- Jeong S. H., Yong S. J., Lee Y. Z. (2007). Friction and wear characteristic due to stick-slip under fretting conditions. *Tribology Transactions*, 50, 564-572.
- Syahirah, M. N., Farhanah, A. N., Bahak M. Z. (2015). Friction and wear of bearing material under water contaminated compressor oil. *Jurnal Tribologi*, 5, 12-22
- Kumar P., Wani M. F. (2017). Friction and wear behaviour of hypereutectic Al-Si alloy/steel tribopair under dry and lubricated conditions. *Jurnal Tribologi*, 15, 21-49
- Fouvry, S., Kapsa, P., & Vincent, L. (1996). Quantification of fretting damage. *Wear*, 200(1-2), 186-205.
- A. Pasanen, A. Lehtovaara, R. Rabb, P. Riihimäki, (1996). Friction behavior of quenched and tempered steel in partial and gross slip conditions in fretting point contact. *Wear*, 267, 2200-2207.